Lattice thermal conductivity reduction in Bi_2Te_3 quantum wires with smooth and rough surfaces: A molecular dynamics study

Bo Qiu, Lin Sun, and Xiulin Ruan*

School of Mechanical Engineering and the Birck Nanotechnology Center,Purdue University,West Lafayette, Indiana 47907-2088, USA

(Received 19 February 2010; revised manuscript received 25 October 2010; published 18 January 2011)

Using molecular dynamics simulations, we have predicted the thermal conductivity of Bi_2Te_3 nanowires with diameters ranging from 3 to 30 nm with both smooth and rough surfaces. It is found that when the nanowire diameter decreases to the molecular scale (below 10 nm, or the so-called "quantum wire"), the thermal conductivity shows significant reduction as compared to bulk value. On the other hand, the thermal conductivity for the 30-nm-diam nanowire only shows less than 20% reduction, in agreement with recent experimental data. Also, the thermal conductivity of nanowires shows a weaker temperature dependence than the typical T^{-1} trend, consistent with experimental observations. This is attributed to the strong boundary scattering of phonons. An analytical model is developed to interpret the molecular dynamics data, and the model suggests that phonon softening in thin nanowires and strong phonon scattering on the rough surface are the two major mechanisms leading to the thermal conductivity reduction. Our results indicate that Bi_2Te_3 nanowires need to be in the molecular scale (diameter below 10 nm) in order to achieve better ZT than the bulk phase.

DOI: 10.1103/PhysRevB.83.035312 PACS number(s): 63.20.dk, 66.70.−f, 71.20.Nr

I. INTRODUCTION

There has been renewed interest in high-performance thermoelectric materials in the past decades. Thermoelectric energy conversion can convert waste heat to electricity without any moving parts; therefore it could play a significant role in addressing the energy challenge. The effectiveness of a thermoelectric material is characterized by its figure of merit ZT, which is determined by three materials properties as $ZT = S^2\sigma T/\kappa$, where S, σ, and T are the Seebeck coefficient, electrical conductivity, and absolute temperature, respectively. Here κ is the thermal conductivity, which contains both electronic and lattice contributions κ_e and κ_l. High-performance thermoelectric materials with high ZT require a high S and σ/κ ratio.

Bi_2Te_3, as well as its alloys, has long been the best thermoelectric material around room temperature with a ZT of about unity. In the past decade, significant enhancement of ZT has been obtained in Bi_2Te_3-based nanostructures, mainly due to the reduced thermal conductivity.[1–7] Among various nanostructures, Bi_2Te_3 nanowires are expected to have reduced thermal conductivity and enhanced ZT as well, and extensive work has been done to synthesize and characterize nanowires with diameters ranging from tens to hundreds of nanometers.[3,8–13] Reduced thermal conductivity has been seen in these experiments, but enhanced ZT is still yet to be found, indicating that the Seebeck coefficient and/or electrical conductivity have deteriorated more. Also, due to different synthesis and characterization methods, the thermal conductivity values for nanowires with diameters of 50–100 nm are not consistent in the literature, ranging from an order of magnitude lower than bulk[9] to only 20% lower than bulk.[3] On the other hand, significantly enhanced ZT has been experimentally demonstrated in silicon nanowires,[14–16] again mainly due to the thermal conductivity reduction up to two orders of magnitude. Since the effective phonon mean free path in bulk silicon is a few hundred nanometers, significant thermal conductivity reduction in 50–100-nm Si nanowire is straightforward. However, as pointed out in Ref. 3, the average phonon mean free path in Bi_2Te_3 bulk phase is already small (about 3 nm at room temperature), and the thermal conductivity reduction in 50–100-nm high-quality single crystalline nanowires should be marginal. It is therefore necessary to evaluate whether Bi_2Te_3 quantum wires with a diameter in the molecular scale can offer further reduction in thermal conductivity.

In this work, we use molecular dynamics (MD) simulations to predict the lattice thermal conductivity of both smooth and rough Bi_2Te_3 nanowires with diameters ranging from 3 to 30 nm. We first study the dependence of lattice thermal conductivity on nanowire diameter at room temperature. Then temperature dependence of both smooth and rough quantum wires with 5.2 nm diameter is examined. By evaluating phonon dispersion relations and density of states (DOS), we observe how the phonon transport is altered, as compared to bulk, in both types of nanowires. By constructing an analytical model and fitting to the MD data, we find that the diameter affects the lattice thermal conductivity through modulating sound velocity and phonon mean free path. We finally use the predicted results to discuss the inconsistencies in the literature and to assess the potential of rough Bi_2Te_3 quantum wires as promising thermoelectric materials.

II. MOLECULAR DYNAMICS SIMULATIONS SETUP

This work mainly concerns diameter and temperature dependencies of thermal conductivity. Two types of cylindrical nanowires, that is, with atomically smooth (SMNW) and sawtooth rough surface (STNW), are considered as shown in Fig. 1. Both nanowires are cut from the bulk phase with axial direction along the bulk [110] direction, which is typical for synthesized Bi_2Te_3 nanowires. The diameter of the STNW is defined as that of its core region, so that its thermal conductivity difference from the SMNW is only due to the rough surface rather than a different core diameter. In experiments, the roughness observed on nanowire surfaces tends to be disordered and randomized with a certain characteristic scale.[3,14] As an approximation, here we construct nanowires with periodic sawtooth-like rough surface as used

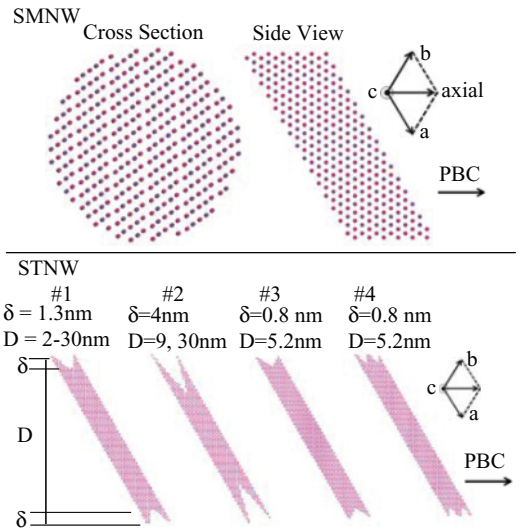

FIG. 1. (Color online) The MD domain setup for cylindrical Bi_2Te_3 nanowires. The a, b, and c axes correspond to the bulk Bi_2Te_3 conventional cell vectors; see Refs. 20 and 21. Periodic boundary conditions are applied in the axial direction. Top panel: SMNW's (cross section and side view); lower panel: STNW's (side view). Blue: Bi atoms; pink: Te atoms.

in earlier Boltzmann Transport Equation (BTE) studies.[17] This type of roughness might not be feasible in experiments due to surface reconstructions. However, the scale of the roughness rather than its shape should be the dominant factor in thermal transport,[14,16–18] thus the sawtooth model is expected to preserve the physics. In the diameter dependence study, the diameter of both SMNW and STNW is generally varied from 3 to 30 nm, while the temperature is fixed at 300 K. For STNW's, two different sawtooth depths of 1.3 nm (No. 1) and 4 nm (No. 2) are considered. In the temperature dependence study, the temperature is varied from 150 to 450 K, while the nanowire diameter is fixed at 5.2 nm. Two different sawtooth densities of 387 teeth/μm (No. 3) and 774 teeth/μm (No. 4) are considered. Since the temperatures under study are higher than the Debye temperature for Bi_2Te_3, which is 155 K,[19] no attempt is made to include quantum corrections.

So far, there are only a few classical interatomic potentials available for Bi_2Te_3, including three-body potentials developed by Huang *et al.*[20] and two-body potentials by us,[21] both of which can reproduce the thermal conductivity of bulk Bi_2Te_3 well; the latter has also been used to successfully predict the thermal conductivity of few-quintuple thin films.[22] We have employed our two-body potentials[21] in this study. Periodic boundary conditions are applied in the axial direction to simulate an infinitely long wire, and at an axial domain length of 2.59 nm, no significant simulation domain size effect is seen. For the radial surface, the free boundary condition is a natural choice to describe free-standing nanowires. However, we have tested both available interatomic potentials and have found that the surface is stable at low temperature but becomes unstable at higher temperatures (such as room temperature). On the other hand, a fixed boundary condition has been used extensively to predict thermal conductivity of nanowires,[23–27] and in the works that compared the two boundary conditions, it was concluded that the fixed boundary condition does not have a significant effect on the resulting thermal conductivity compared to the free boundary condition. Therefore, the fixed boundary condition is used here. It not only directly mimics nanowires embedded in an environment with very different elastic properties, such as those Bi_2Te_3 nanowires grown in porous template,[9] but also should yield results that are comparable to experimental data on freestanding nanowires.

The thermal conductivity is simulated using equilibrium MD with the Green-Kubo theory.[28] For a pair potential, the heat current vector is expressed as

$$\mathbf{S} = \frac{1}{2}\sum_{i,j}(\mathbf{F}_{ij}\cdot\mathbf{v}_i)\mathbf{r}_{ij,o}, \tag{1}$$

where $\mathbf{v}_i$ is the velocity of atom i and $\mathbf{F}_{ij}$ is the force between atoms i and j. In a solid, since atoms vibrate locally, the heat current $S(t)$ can be expressed in terms of the equilibrium interatomic separations between atom i and j, noted as $\mathbf{r}_{ij,o}$. The thermal conductivity can then be calculated from the autocorrelation function of the heat current.[29] Note that nanowire is an anisotropic system; the thermal conductivity in the axial direction is totally different from that in the radial direction. To calculate the axial thermal conductivity, only the axial component of the heat current vector should be used in the autocorrelation function, that is,

$$\kappa_{l,c} = \frac{1}{k_B V T^2}\int_0^\infty \langle S_c(t)S_c(0)\rangle dt, \tag{2}$$

where V is the volume of simulation domain, T is the temperature, and $\langle S_c(t)S_c(0)\rangle$ is the axial direction heat current autocorrelation function (HCACF). The subscript c indicates the axial component. With the time step chosen to be 1.23 fs, the system is first run in an NVT ensemble for 120 ps to ensure equilibration, then switched to an NVE ensemble for 1080 ps. The heat current is extracted in the last 960 ps of the NVE ensemble and the HCACF is obtained through postprocessing. The direct integrals of HCACF show a plateau between 10 and 20 ps then occasionally diverge afterwards. This is commonly seen due to the statistically fluctuating nature of MD simulations,[30–32] usually making the calculation of thermal conductivity ambiguous. In the present work, instead of performing the direct integral in Eq. (2), we first apply the appropriate Fourier filter to the HCACF and fit an exponential decay function to the filtered HCACF. We can then conveniently evaluate the integral of the fitted exponential function. Details of the procedure can be found in our previous work.[21,22] For each temperature or diameter, 15 runs of independent MD simulations with randomized initial momentum are carried out and averaged to minimize statistical fluctuations.

III. RESULTS AND DISCUSSION

A. Effects of diameter and roughness on thermal conductivity

The lattice thermal conductivities of SMNW's and STNW's (No. 1 and No. 2) as a function of diameter are plotted in Fig. 2. For SMNW's, κ_l decreases with decreasing diameter down to 4 nm. The κ_l of STNW's decreases monotonically with

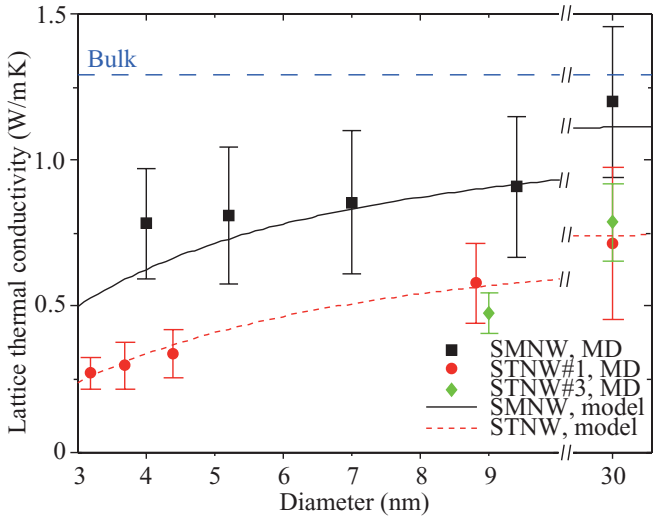

FIG. 2. (Color online) Predicted lattice thermal conductivity of SMNW's and STNW's at room temperature as a function of diameter. The results from the analytical model are also shown as a comparison.

decreasing diameter, and is generally at least 25% less than that of SMNW's. When nanowire diameter is larger, the difference in thermal conductivity between SMNW and STNW, as well as between STNW No. 1 and No. 2, is smaller. This suggests that the axial phonon transport experiences less scattering at the boundaries and has less sensitivity on the conditions of surface roughness in thicker nanowires.

Overall, the thermal conductivity of SMNW's with diameters below 10 nm is reduced by 30%–40% compared to bulk, while more than 55% reduction is found in STNW's. Such a reduction likely comes from the fact that thickness of surface roughness serves as a second scattering scale in addition to nanowire diameter and efficiently hinders the transport of higher frequency acoustic phonons. So far we cannot directly validate these prediction data against experiments since thermal conductivity has not been measured on Bi_2Te_3 nanowires with diameters below 10 nm. For validation purposes, we have performed additional simulations for 30-nm-diam nanowires, also shown in Fig. 2. The κ_l is found to be around 0.75 W/m K for STNW No. 1 and No. 2 and 1.2 W/m K for SMNW, representing 42% and 8% reductions from the bulk value, respectively. The trends are in good agreement with the 20% reduction found by Mavrokefalos *et al.* in a 52-nm-diam freestanding bismuth telluride nanowire with rough surface.[3] This agreement also indicates that the fixed or free boundary condition does not affect thermal conductivity much. It is noted that over an order of magnitude reduction in thermal conductivity was reported in an earlier measurement on electrodeposited bismuth telluride nanowires with 40 nm diameter embedded in amorphous alumina.[9] This extremely low value is unlikely to be due to boundary scattering only, since the phonon mean free path in bulk is only a few nanometers at room temperature. Instead, point defects, impurities, grain boundaries (in polycrystal nanowires), and nonuniform composition might be responsible.

For silicon nanowires, it was found that surface roughness on the scale of several nanometers can bring down the thermal conductivity by an order of magnitude.[14,15] Note that bulk silicon has thermal conductivity of about 149 W/m K with phonon mean free path around 200 nm at room temperature. Unlike silicon, κ_l is only around 1.5 W/m K in bulk Bi_2Te_3, and the phonon mean free path is only about 8 nm at room temperature. Therefore, the impact of boundary and roughness scattering on Bi_2Te_3 nanowire thermal conductivity is much smaller, as confirmed by the only slight reduction seen in our predicted data on 30-nm-diam nanowires and experimental data on 50-nm nanowires in Ref. 3. One has to use molecular scale nanowires (diameter below 10 nm) or introduce other scattering mechanisms such as impurity and defect scattering in order to observe significant thermal conductivity reduction, as also pointed out in Ref. 33.

B. Temperature dependence of thermal conductivity

The thermal conductivities κ_l of 5.2-nm-diam SMNW, STNW No. 3, and STNW No. 4 as a function of temperature are shown in Fig. 3, along with the in-plane thermal conductivity values of bulk from experiments and prior simulations using the same interatomic potentials.[21] Overall, κ_l of SMNW's shows a reduction by 50% in average as compared to the predicted bulk value, while κ_l of STNW's shows an additional 35% reduction from that of SMNW's over the temperature range 150–450 K. Considering the broad temperature range as well as the small thickness of sawtooth-like surface roughness in the present work (~1 nm), the amount of additional κ_l reduction in STNW's is remarkable. On the other hand, by comparing STNW's with different sawtooth densities, it is found that κ_l of STNW No. 4 is only 5% lower than that of STNW No. 3 on average, indicating that the sawtooth density has limited impact on phonon scattering.

Also, from bulk to SMNW's and to STNW's, the temperature dependence of κ_l gradually weakens and deviates from the T^{-1} trend, indicating that Umklapp scattering in bulk becomes less important in nanowires. According to

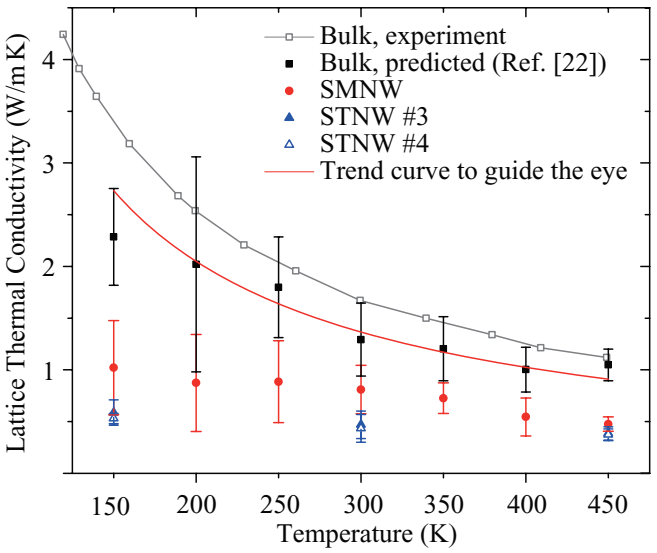

FIG. 3. (Color online) The lattice thermal conductivities of 5.2-nm-diam SMNW's, STNW No. 3, and STNW No. 4 as a function of temperature, in comparison with bulk values from both simulations (Ref. 21) and experiments (Ref. 34).

classical kinetic theory, the intrinsic phonon mean free path l_b has temperature dependence $l_b \propto \kappa \propto T^{-1}$ in bulk. As a result, l_b is higher at lower temperatures. In SMNW's, the finite dimension in the radial direction introduces boundary scatterings, which are largely independent of temperature. The combined effect of Umklapp and boundary scattering leads to a weaker temperature dependence than T^{-1}. As a result, thermal conductivity reduction in nanowires is more evident at low temperature. Such behavior is more apparent in STNW's, where the additional scatterings at rough nanowire surfaces are also temperature independent. The weakened temperature dependence was also observed in recent experiments on bismuth telluride nanowires with diameters around 52–55 nm,[3] and on various other nanowire systems.[35–37]

C. Phonon dispersion relation and vibrational spectra

As mentioned above, finite dimensions in the radial direction of nanowires can introduce strong phonon confinements, leading to reduction in sound velocities. The reduction in lattice thermal conductivity of Bi_2Te_3 nanowires can be partially attributed to such phonon confinements. To verify this argument, we perform lattice dynamics (LD) calculations to obtain the phonon dispersions of 5.2-nm-diam SMNW using the GULP package.[38] According to Khitun *et al.*,[25] differences in group velocities due to the use of free and clamped boundary conditions are small, especially for those low-frequency acoustic phonons that carry the majority of heat. Despite stability issues of nanowires at higher temperatures with adopted potentials under free boundary conditions, the system is stable in LD calculations, which corresponds to 0 K. Therefore, we are able to use LD calculations for nanowire structures without any fixed atoms to allow for surface relaxation. After geometry optimization, we compute phonon dispersion relations then zoom in on the low-frequency regime, as shown in Fig. 4(a). It is seen that, as opposed to bulk, there are four acoustic phonon branches, which are characteristic for nanowires.[39,40] Two of these branches are linear in wave vector q and can be identified as the longitudinal and transverse acoustical phonons. The transverse phonon is a torsional mode in the wire. Furthermore, two branches proportional to q^2 can be observed, corresponding to a bending of the wire. As compared to bulk Bi_2Te_3, softening of the lowest acoustic phonon branches in nanowires is evident. Such a phonon-softening phenomenon can originate from the loss of neighbors (free surface) or proximity to immobile neighbors (immersed system or fixed boundary) for surface atoms, or dissimilarity of force constants for atoms at material interfaces. In all cases, a local environment different from that in bulk will be created, which alters the atomic vibration pattern, usually leading to lowered sound velocities. Similar trends have also been observed in Y_2O_3 nanostructures.[41]

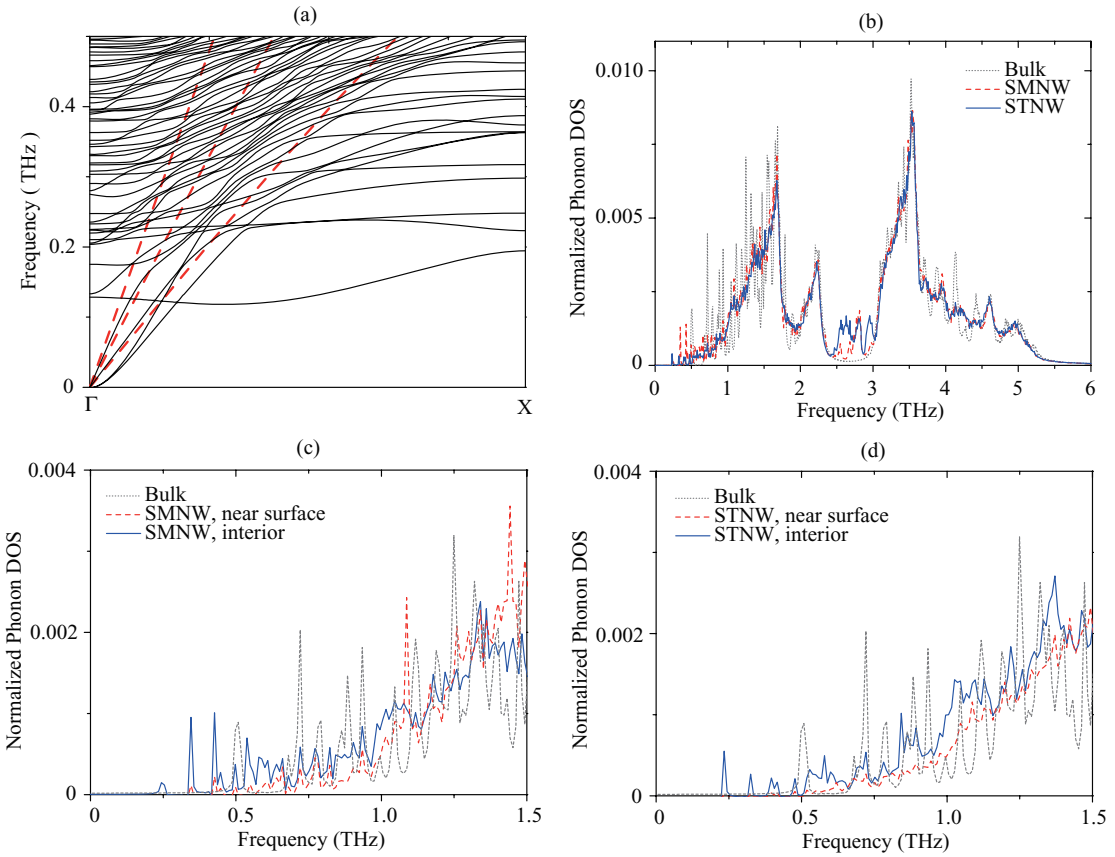

FIG. 4. (Color online) (a) Phonon dispersions of 5.2-nm-diam SMNW along the axial direction in comparison with three acoustic phonon branches of bulk (shown by red dotted lines). (b) Comparison between the total phonon DOS of bulk, SMNW, and STNW. (c) Local phonon DOS of SMNW near surface and interior regions in comparison with bulk. (d) Local phonon DOS of STNW near surface and interior regions in comparison with bulk.

In addition, the phonon density of states are calculated as the Fourier transforms of the normalized velocity autocorrelation function,

$$\Gamma(t) = \left\langle \sum_{i=1}^{N} v_i(t)v_i(0) \right\rangle \Big/ \left\langle \sum_{i=1}^{N} v_i(0)v_i(0) \right\rangle, \qquad (3)$$

which can be directly extracted from MD simulations. Here v_i is the velocity of atom i, and the summation can be done on a particular region, species, or all atoms in the system. More details of how to calculate and interpret various types of partial phonon DOS have been given in our previous work.[41] The computed total phonon DOS of both SMNW's and STNW's are plotted in comparison with that of bulk in the [110] direction in Fig. 4(b). As seen, the phonon spectra in both nanowires are generally broadened, which is a result of redistribution of phonon states due to lowered symmetry in the presence of a surface.[41,42] The phonon DOS at low-frequency regions are enhanced due to the softening of bonds among atoms near the surface. Those peaks between 2.5 and 3 THz found in both types of nanowire are due to phonon DOS contributions from surface, possibly indicating the localization of phonons in the surface regions.[15] The lack of high-frequency tails is possibly due to the use of fixed boundary conditions, which stops nanowire from shrinking.[43] However, since optical phonons at the high-frequency end do not contribute much to thermal conductivity, omitting this part is not expected to affect the κ_l value.[44] It is also noted that although fixed boundary condition is used in this work, the DOS shows very similar feature with that derived under free boundary conditions,[41] indicating that the fixed boundary condition does not alter the phonon behavior significantly.

Since the majority of heat is carried by acoustic phonons in Bi_2Te_3, we take a closer look at the zoom in on the DOS in the acoustic regions below 1.5 THz for SMNW and STNW, as shown in Figs. 4(c) and 4(d), respectively. In the rest of the discussion in this section, we use "number of states" to refer to the relative number of phonon states in acoustic range against that in full phonon spectrum. From the plots, it is seen that low-frequency peaks that do not exist in bulk DOS are found in both SMNW and STNW. It is also interesting to note that these peaks mostly exist in interior regions for both types of nanowires, indicating that the strong phonon confinements and surface conditions in fact largely alter the internal phonon transport. Such peaks also imply the shrinking of the extent of acoustic phonon modes, which leads to reduced group velocity and thus lower lattice thermal conductivity,[45] as compared to bulk. Also, by comparing the phonon DOS of two types of nanowire, it is found that the number of available phonon states in STNW is less than that in SMNW in the acoustic region, indicating that the heat conduction in STNW is worse. The impacts of surface conditions can be better viewed by comparing relative contributions of phonon states to total thermal transport from interior and near-surface regions in both types of nanowire. For SMNW's, the number of phonon states in the interior region is higher for frequencies around and below 1 THz. Since the majority of heat is carried through interior regions, a larger number of states in the interior region favors heat conduction. Therefore, despite the presence of system boundaries, phonon transport along the SMNW axial direction is relatively less disturbed, leading to moderate thermal conductivity. On the other hand, available phonon states in the interior region are as few as in the near-surface region in STNW's for the low-frequency regime. This indicates that the existence of surface roughness strongly enforces the redistribution of phonon states, leading to an overall quench of available states for heat conduction, resulting in heavily suppressed thermal conductivity.

D. An analytical model for diameter dependence of thermal conductivity

To interpret the effects of nanowire diameter and roughness on thermal conductivity, we propose an analytical model based on the kinetic theory $\kappa_l = (1/3)cv_s^2\tau$, where c is the specific heat capacity, v_s is the sound velocity, and τ is the effective phonon relaxation time. We assume τ to be in the form of

$$\frac{1}{\tau} = \frac{1}{\tau_U} + \frac{1}{\tau_B} + \frac{1}{\tau_\delta}, \qquad (4)$$

where τ_U, τ_B, and τ_δ denote the relaxation times for Umklapp, boundary, and surface roughness scattering processes, respectively. τ_B can be written as

$$\tau_B = \frac{\tau_U}{\left(\frac{1-p}{1+p}\right)(l_0/D)}, \qquad (5)$$

where l_0 is the phonon mean free path in bulk, D is the nanowire diameter, and p is the specularity parameter that reflects the boundary scattering conditions, with a value between 0 (diffusive) and 1 (specular). For surface roughness scattering, Martin *et al*. observed that phonon scattering rate has a quadratic dependence on the roughness δ in rough silicon nanowires.[16] Therefore we assume

$$\tau_\delta = \frac{\tau_U}{B_{\rm st}(\delta/D)^2}, \qquad (6)$$

where $B_{\rm st}$ is a parameter associated with the roughness scattering strength (the larger, the stronger), which depends on both the material and the geometry of roughness. On the other hand, v_s is related to cohesive energy E_c under the isotropic continuum approximation,[46] that is,

$$v_s^2 \propto E_c \propto \left(1 - \frac{1}{12D/L_0 - 1}\right) \exp\left(-\frac{2S_m}{3R}\frac{1}{12D/L_0 - 1}\right), \qquad (7)$$

which is assumed to hold for Bi_2Te_3 nanowires along the axial direction. Here, S_m is the bulk melting entropy, R is the ideal gas constant, and $L_0 = 4w$ is a critical size at which almost all atoms are localized at the nanowire surface,[47] where w is the atomic/molecular diameter. Furthermore, a correction term $p\exp(-\alpha l_0/D)$ is included for the effects from the nonequilibrium phonon distribution due to rough boundaries, as suggested by Liang and Li.[47] Here α is taken to be 1/3 for Bi_2Te_3 quantum wires. In the end, by combining τ, v_s, and assuming c to take its bulk value, an analytical model for κ_l of rough nanowires is reached as

$$\kappa_l = \kappa_0 p \exp(-\alpha l_0/D) \times \frac{\left(1 - \frac{1}{12D/L_0 - 1}\right) \exp\left(-\frac{2S_m}{3R}\frac{1}{12D/L_0 - 1}\right)}{1 + \left(\frac{1-p}{1+p}\right)(l_0/D) + B_{\rm st}(\delta/D)^2}, \qquad (8)$$

TABLE I. Summary of nonfitting parameters used in Eq. (8) for Bi_2Te_3 nanowires.

S_m (J mol^{-1} K^{-1})	w (nm)	l_0 (nm)	δ (nm)
36.2	0.44	6.0	1.3 (ST); 0 (SM)

where κ_0 is the lattice thermal conductivity of bulk Bi_2Te_3 at room temperature. The only fitting parameters in this model are p and B_{st} while all others can be obtained from materials properties and system geometry, as summarized in Table I.

The derived analytical model is based on averaged sound velocities and relaxation times, and is therefore much simpler in the sense of computing phonon relaxation times, compared to some models for surface roughness in silicon nanowires involving frequency-resolved representations.[16] In comparison with Liang and Li's model on semiconducting nanowires,[47] our analytical model has an additional term to account for surface roughness scatterings; thus it can be successfully fitted to experimental values on silicon nanowires with various degrees of surface roughness.[8,14] In the present work, this analytical model is fitted to the MD data we obtained for Bi_2Te_3 nanowires at room temperature. By taking into account the temperature dependence of l_0 and κ_0, the model is likely to be extended to temperatures other than 300 K. As a side note, the fitted parameters are only intended to be good for the data they are fitted to.

Best fittings to MD data are achieved with $p = 0.94$, $B_{st} = 0$ and $p = 0.74$, $B_{st} = 1.6$ for SMNW's and STNW's, respectively, indicating that STNW's have more diffusive boundaries and stronger roughness scatterings. The fitting of the analytical model to MD data of κ_l is shown in Fig. 2, and v_s and τ from the analytical model are shown in Figs. 5(a) and 5(b), respectively. As seen, the sound velocity is generally smaller in nanostructures than in bulk. To confirm the validity of the analytical model, sound velocity of SMNW's of various diameters is extracted from LD calculations in combination with the Debye approximation for comparison, following the procedures mentioned in previous sections. As seen in Fig. 5(a), despite the difference in sound velocity values due to the use of Debye model,[25] qualitative agreement in trends is found between LD calculation and the analytical model, which validates the analytical model. The predicted sound velocity v_s generally decreases with decreasing diameter for both types of nanowire, which is expected due to stronger phonon confinements in thinner nanowires. In addition, the v_s values of STNW's are 16% smaller than those of SMNW's in general. This indicates that besides the strong phonon softening of low-frequency phonon modes at smaller diameters due to one-dimensional (1D) confinement structures, surface roughness further hinders phonon propagation by additional scattering and by creating phonon localizations, which agrees with Donadio and Galli's observations in rough Si nanowires.[15] In Fig. 5(b), τ in STNW's drops rapidly below 4 nm, indicating that an increasingly significant portion of phonons are strongly scattered at the surface when nanowire diameter approaches the scale of the roughness. Such behavior originates from the fact that with smaller diameters, the nanowire interior region shrinks, leading to a larger portion of phonons transported through near-surface regions, and thus strongly scattered or localized. In contrast, the analytical model indicates that τ values of SMNW's should be smaller but close to that in bulk due to the near-specular boundary, since the surfaces of SMNW's are nearly atomically smooth.

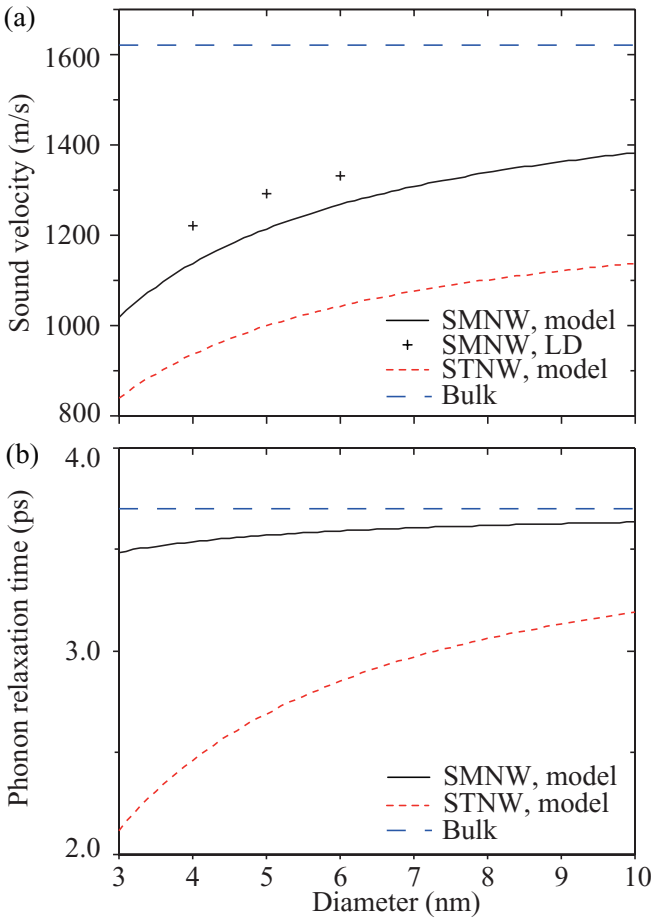

FIG. 5. (Color online) (a) Sound velocity of SMNW's and STNW's produced by an analytical model, along with that obtained from lattice dynamics calculations for SMNW's. (b) Average phonon relaxation time of SMNW's and STNW's produced by an analytical model.

IV. CONCLUSIONS

In summary, MD simulations have been performed to predict the lattice thermal conductivity of thin Bi_2Te_3 nanowires at different diameter, temperature, and surface roughness. It is found that with the shrinkage of the nanowire diameter, the thermal conductivity is greatly reduced for thin rough nanowires with diameters below 10 nm, while the thermal conductivity is only slightly reduced for diameters higher than 30 nm. It is also found that the temperature dependence weakens from bulk to nanowires due to the decreasing importance of the Umklapp process. Over the temperature range 150–450 K, with a 5.2 nm diameter, κ_l can be significantly reduced by as much as 50% in smooth nanowires due to 1D phonon confinement effects, while additional reduction of around 35% can result from surface roughness. Phonon dispersions are altered in the sense of softened acoustic phonon

branches, which leads to reduced sound velocity. The density of available phonon states is forced to redistribute among low-frequency regimes depending on surface conditions. An analytical model based on averaged sound velocity and phonon relaxation time with a few fitting parameters is proposed to interpret the diameter and roughness dependence of κ_l of Bi_2Te_3 nanowires. It is found that in SMNW's, the main cause for the reduction of κ_l is the drop in sound velocity due to strong phonon confinement. In STNW's, the drop of κ_l is due to combined effects of both reduction of sound velocity and strong phonon scattering or localization at rough surface. Our work indicates that molecular-scale rough Bi_2Te_3 nanowires are very promising thermoelectric materials.

ACKNOWLEDGMENTS

This work was partly supported by a faculty startup fund from Purdue University. B. Qiu also acknowledges the support from the School of Mechanical Engineering, Purdue University.

*ruan@purdue.edu

[1] R. Venkatasubramanian, E. Siivola, T. Colpitts, and B. O'Quinn, Nature **413**, 597 (2001).
[2] B. Poudel *et al.*, Science **320**, 634 (2008).
[3] A. Mavrokefalos, A. L. Moore, M. T. Pettes, L. Shi, W. Wang, and X. Li, J. Appl. Phys. **105**, 104318 (2009).
[4] D. Teweldebrhan, V. Goyal, and A. A. Balandin, Nano Lett. **10**, 1209 (2010).
[5] C. Chen, Y. Chen, S. Lin, J. C. Ho, P. C. Lee, C. D. Chen, and S. R. Harutyunyan, J. Phys. Chem. C **114**, 3385 (2010).
[6] M. Takashiri, M. Takiishi, S. Tanaka, K. Miyazaki, and H. Tsukamoto, J. Appl. Phys. **101**, 074301 (2007).
[7] D. Kim, E. Byon, G. Lee, and S. Cho, Thin Solid Films **510**, 148 (2006).
[8] D. Li, Y. Wu, P. Kim, L. Shi, P. Yang, and A. Majumdar, Appl. Phys. Lett. **83**, 2934 (2003).
[9] D. A. Borca-Tasciuc, G. Chen, A. Prieto, M. S. Martin-Gonzalez, A. Stacy, T. Sands, M. A. Ryan, and J. P. Fleurial, Appl. Phys. Lett. **85**, 6001 (2004).
[10] H. Yu, P. C. Gibbons, and W. E. Buhro, J. Mater. Chem. **14**, 595 (2004).
[11] J. Zhou, C. Jin, J. H. Seol, X. Li, and L. Shi, Appl. Phys. Lett. **87**, 133109 (2005).
[12] E. J. Menke, M. A. Brown, Q. Li, J. C. Hemminger, and R. M. Penner, Langmuir **22**, 10564 (2006).
[13] K. G. Biswas, T. D. Sands, B. A. Cola, and X. Xu, Appl. Phys. Lett. **94**, 223116 (2009).
[14] A. I. Hochbaum, R. Chen, R. D. Delgado, W. Liang, E. C. Garnett, M. Najarian, A. Majumdar, and P. Yang, Nature **451**, 163 (2008).
[15] D. Donadio and G. Galli, Phys. Rev. Lett. **102**, 195901 (2009).
[16] P. Martin, Z. Aksamija, E. Pop, and U. Ravaioli, Phys. Rev. Lett. **102**, 125503 (2009).
[17] A. L. Moore, S. K. Saha, R. S. Prasher, and L. Shi, Appl. Phys. Lett. **93**, 083112 (2008).
[18] P. Martin, Z. Aksamija, E. Pop, and U. Ravaioli, Nano Lett. **10**, 1120 (2010).
[19] G. E. Shoemake, J. A. Rayne, and R. W. U. Jr., Phys. Rev. **185**, 1046 (1969).
[20] B. L. Huang and M. Kaviany, Phys. Rev. B **77**, 125209 (2008).
[21] B. Qiu and X. Ruan, Phys. Rev. B **80**, 165203 (2009).
[22] B. Qiu and X. Ruan, Appl. Phys. Lett. **97**, 183107 (2010).
[23] J. Carrete, R. C. Longo, L. M. Varela, J. P. Rino, and L. J. Gallego, Phys. Rev. B **80**, 155408 (2009).
[24] P. Chantrenne and J. L. Barrat, J. Heat Transfer **126**, 577 (2004).
[25] A. Khitun, A. Balandin, and K. L. Wang, Superlatt. Microstruct. **26**, 181 (1999).
[26] S. G. Volz and G. Chen, Appl. Phys. Lett. **75**, 2056 (1999).
[27] S. Volz, D. Lemonnier, and J. B. Saulnier, Nanoscale Microscale Thermophys. Eng. **5**, 191 (2001).
[28] R. Kubo, M. Toda, and N. Hashitsume, *Statistical Physics II, Nonequilibrium Statistical Mechanics* (Springer-Verlag, Berlin, 1991).
[29] D. A. McQuarrie, *Statistical Mechanics* (University Science Books, Sausalito, CA, 2000).
[30] A. J. H. McGaughey and M. Kaviany, Int. J. Heat Mass Transf. **47**, 1799 (2004).
[31] H. Ishii, A. Murakawa, and K. Kakimoto, J. Appl. Phys. **95**, 6200 (2004).
[32] B. L. Huang and M. Kaviany, Acta Mater. **58**, 4516 (2010).
[33] H. W. Hillhouse and M. T. Tuominen, Microporous Mesoporous Mater. **47**, 39 (2001).
[34] C. B. Satterthwaite and J. R. W. Ure, Phys. Rev. **108**, 1164 (1957).
[35] C. C. Yang and S. Li, Phys. Rev. B **75**, 165413 (2007).
[36] A. I. Boukai, Y. Bunimovich, J. Tahir-Kheli, J. Yu, W. A. G. III, and J. R. Heath, Nature **451**, 168 (2008).
[37] M. Fardy, A. I. Hochbaum, J. Goldberger, M. M. Zhang, and P. Yang, Adv. Mater. **19**, 3047 (2007).
[38] J. D. Gale, J. Chem. Soc. Faraday Trans. **93**, 629 (1997).
[39] T. Thonhauser and G. D. Mahan, Phys. Rev. B **69**, 075213 (2004).
[40] H. Peelaers, B. Partoens, and F. M. Peeters, Nano Lett. **9**, 107 (2009).
[41] H. Bao, X. L. Ruan, and M. Kaviany, Phys. Rev. B **78**, 125417 (2008).
[42] S. R. Calvo and P. B. Balbuena, Surface Sci. **581**, 213 (2005).
[43] X. L. Ruan and M. Kaviany, Phys. Rev. B **73**, 155422 (2006).
[44] J. V. Goicochea, M. Madrid, and C. Amon, J. Heat Transfer **132**, 012401 (2009).
[45] A. J. H. McGaughey, M. I. Hussein, E. S. Landry, M. Kaviany, and G. M. Hulbert, Phys. Rev. B **74**, 104304 (2006).
[46] C. C. Yang, J. Armellin, and S. Li, J. Phys. Chem. B **112**, 1482 (2008).
[47] L. H. Liang and B. Li, Phys. Rev. B **73**, 153303 (2006).